ChemPubSoc Europe

DOI: 10.1002/cphc.201402207

On the Origin of Damped Electrochemical Oscillations at Silicon Anodes (Revisited)

Joris Proost,*[a] Frédéric Blaffart,[a] Stuart Turner,[b] and Hosni Idrissi[a, b]

Electrochemical oscillations accompanying the formation of anodic silica have been shown in the past to be correlated with rather abrupt changes in the mechanical stress state of the silica film, commonly associated with some kind of fracture or porosification of the oxide. To advance the understanding on the origin of such oscillations in fluoride-free electrolytes, we have revisited a seminal experiment reported by Lehmann almost two decades ago. We thereby demonstrate that the oscillations are not stress-induced, and do not originate from a morphological transformation of the oxide in the course of anodisation. Alternatively, the mechanical features accompanying the oscillations can be explained by a partial relaxation of the field-induced electrostrictive stress. Furthermore, our observations suggest that the oscillation mechanism more likely results from a periodic depolarisation of the anodic silica.

1. Introduction

■■Please give academic titles of the authors■■A remarkable and intriguing feature of silicon anodising is the oscillatory behaviour that occurs spontaneously in various regimes of anodic silica growth. In dilute fluoride-containing electrolytes, silicon electrodissolution can lead to sustained potential or current oscillations under galvanostatic and potentiostatic conditions, respectively.[1,2] These oscillations can be taken as indicative of both temporal and spatial inhomogeneities in the oxide growth mechanism. As for the latter, two fundamentally different viewpoints currently exist within the scientific community on the origin of stable oscillations. On the one hand, there is the picture of coupled, self-oscillating domains,[3] whereas on the other hand there is the viewpoint of a homogeneous oscillatory medium.[4] In both cases, the so-called base oscillator is usually associated with periodic morphological variations of the anodic silica, which affect properties such as thickness, roughness and mechanical stress.[5–8] In fluoride-free electrolytes, that is, in the absence of silica dissolution, damped oscillations are generally observed during anodic silica growth.[1,9] These damped oscillations show very similar features to sustained oscillations. For instance, in galvanostatic experiments, periodic potential drops have been observed in both regimes to occur simultaneously with periodic changes in internal stress.[7,10] A better understanding of this seemingly common mechanical behaviour therefore appears to be of primary importance to advance the understanding of the anodic silica growth mechanism.

As a result, based on the above experimental observations, various models have been proposed in the literature[9,11,12] that include a mechanical component in one way or another for describing the oscillatory component characteristic for anodic silica growth. Their common feature is the consideration that the oscillations are associated with some kind of stress-induced morphological transformation of the anodic oxide film, such as fracture or porosification. This hypothesis is often motivated by referring to a seminal experiment carried out by Volker Lehmann almost two decades ago.[13] He has been the first to resolve a characteristic increase of internal stress in the compressive direction accompanying the periodic potential drops during galvanostatic oxide growth in fluoride-free electrolytes. Based on his combined electromechanical observations, carried out for the first time in situ during oxide growth, Lehmann then claimed the oscillation process to be based on a stress-induced, dense-to-porous transition of the anodic oxide morphology.

The main objective of this article is to revisit Lehmann's seminal experiment, thereby benefiting from significant instrumental improvements that have been realised over the past decade within our group for in situ stress and thickness monitoring during anodic oxide growth. Moreover, we have combined these high-resolution in situ measurements with a detailed ex situ structural characterisation using atomic force microscopy (AFM) and high-resolution cross-sectional transmission electron microscopy (TEM). As a result, we have been able on the one hand to carefully reproduce Lehmann's experimental findings, but on the other hand to disprove his claim of a stress-induced morphological transition. Alternatively, we attribute the periodic stress transitions in the compressive direction to a relaxation of the tensile, field-induced electrostrictive stress component in the silica film, which results from a periodically relaxing electrical field. The origin of the oscillation there-

[a] J. Proost, F. Blaffart, H. Idrissi
Institute of Mechanics, Materials and Civil Engineering
Université Catholique de Louvain
Place Sainte-Barbe 2, 1348 Louvain-la-Neuve (Belgium)
E-mail: joris.proost@uclouvain.be

[b] S. Turner, H. Idrissi
Department of Physics, University of Antwerp
Groenenborgerlaan 171, 2020 Antwerp (Belgium)

fore rather appears to be electrical in nature, which we imagine as a periodic charge dissipation within the oxide.

Experimental Section

Anodising Setup

The anodic silica film grows on a cantilevered silicon anode designed for the combined use of in situ spectroscopic ellipsometry (Smart SE from Jobin Yvon) and in situ multi-beam optical stress sensing (MOSS from k-Space Inc.). The combination of these two in situ diagnostic probes allows monitoring of the evolution of both the thickness and the internal stress in real time during anodic silica growth, as has already been described in detail elsewhere.[14] In short, the film thickness evolution was determined by fitting the recorded ellipsometric spectrum in the range 450–900 nm with a three-layer optical model, in which the growing anodic silica is represented as a transparent Cauchy layer. Spectral fitting was found to yield the best results by assuming the silica refractive index to remain constant during growth. This assumption has been verified a posteriori by ex situ TEM characterisation of the films, as will be presented in the Results section below.

The MOSS uses a charge-coupled device to detect the centroid positions of the reflections of a series of parallel laser beams coming off the anode back side. It thereby allows monitoring of changes in substrate curvature $\Delta\kappa$ with both high radius (10 km) and temporal (0.1 s) resolution. These changes are proportional to the product of the average biaxial internal stress $<\sigma_f>$ in the silica film and its thickness h_f, according to the well-known Stoney equation [Eq. (1)]:[15]

$$\langle\sigma_f\rangle \cdot h_f = \left(\frac{Y}{1-\nu}\right)_s \cdot \frac{h_s^2}{6} \cdot \Delta\kappa \qquad (1)$$

in which Y_s, ν_s and h_s are the Young modulus, Poisson ratio and thickness of the silicon substrate, respectively.

Samples and Methods

Room-temperature galvanostatic anodising experiments were performed at current densities j varying between 0.07 and 0.13 mA cm^{-2} in 10% acetic acid, prepared from analytical grade glacial acetic acid (Fisher) and ultrapure water (resistivity >18 MΩ cm). The 50 mm × 4 mm silicon cantilevers were cut from double-side polished, (100)-oriented silicon wafers with a nominal thickness of 200 μm. The p-doped Si had a resistivity of 10 ± 5 Ω cm, and electrical contact was ensured by the deposition of 300 nm of aluminium. The back side of the samples was passivated with 100 nm of low-pressure chemical vapour deposited (LPCVD) Si_3N_4, whereas on the front surface, a stripe of the same LPCVD Si_3N_4 was deposited at the electrolyte/air interface. This prevented a change in meniscus position at the start of silica growth, which has been shown in the past to be a possible source of error during the initial curvature–stress calculation.[10]

Cross-sectional TEM lamellae were prepared from cut-outs of anodised cantilevers by focused ion beam (FIB) in an FEI Helios FIB scanning electron microscope■■OK?■■. To prevent any surface damage, a protective electron-beam-deposited platinum (Pt) film was deposited on top of the silica layers, followed by the deposition of an ion-beam Pt layer prior to FIB milling. The microstructure of the silica layers was then investigated using an FEI Titan 80–300 "cubed" transmission electron microscope, operated at 300 kV and equipped with probe and image aberration correctors, as well as a Quantum Gatan energy filter (GIF) for electron energy-loss spectroscopy (EELS). High-angle annular dark-field scanning transmission electron microscopy (HAADF-STEM) imaging was carried out using a convergence semi-angle α of 22 mrad and an acceptance inner semi-angle β to ensure HAADF-STEM conditions. EELS data were acquired in STEM mode using a collection semi-angle β of 36 mrad. The HAADF-STEM intensity plots were summed over the full displayed image width. Quantification of the Si/O ratio was performed using standard quantification techniques in the Digital Micrograph (DM) software package. Finally, AFM surface characterisations were performed in tapping mode on samples anodised to different growth stages. The AFM tips had a nominal resonant frequency of 330 kHz and an apex radius lower than 10 nm.

2. Results

Figure 1 compares Lehmann's reference experiment (Figure 1 a),[13] which was carried out at 0.10 mA cm^{-2}, with our own reproduction (Figure 1 b) on similar ordinate and abscissa scales. The two sets of curves show a strikingly similar evolution for the voltage, thickness and stress (or rather stress*thickness)■* OK?■ signals, including the same periodic transitions. These transitions are characterised by a rather abrupt potential drop, an increase in growth rate and a pronounced increase of the internal stress in the compressive direction. The amplitude and the rate of these transitions decrease at each cycle, and the oscillations become fully damped after four cycles, as shown in Figure 1 c. Note the significantly improved time resolution of both the thickness and curvature signals in our reproduced experiment, especially at the transitions, as compared to the discrete points in Lehmann's observations. This is especially pronounced for the thickness signal in Figure 1 a (open circles), which completely misses the second to fourth oscillations.

Figure 2 shows the evolution of the cell potential and thickness at different current densities. The oscillation frequency increases with current density, and each transition occurs after a fixed amount of charge has passed, equal to 250 ± 13 mC cm^{-2}. This corresponds to a measured thickness increment of 11.8 ± 0.1 nm per cycle. In between the transitions, there is a non-linear increase in both potential and thickness. It is fast at the beginning of the cycle, but then progressively slows down until the next transition occurs. At the transition itself, the voltage and thickness evolutions are not fully synchronised. Indeed, the enlargement at the transition displayed in Figure 3 shows that the increase of the growth rate occurs several tens of seconds after the onset of the potential drop. This suggests that the increase in growth rate is a consequence of the potential drop. Also note in Figure 3 the quantitative agreement between our own continuous thickness measurement, carried out in situ by spectroscopic ellipsometry, and discrete thickness measurements performed independently by other groups ex situ for similar anodising conditions, and represented in Figure 3 by discrete circles (from ref. [13]) and squares (from ref. [9]). This provides confidence to our ellipsometric data extraction procedure, which, besides the thickness evolution, also allowed us to independently obtain the refrac-

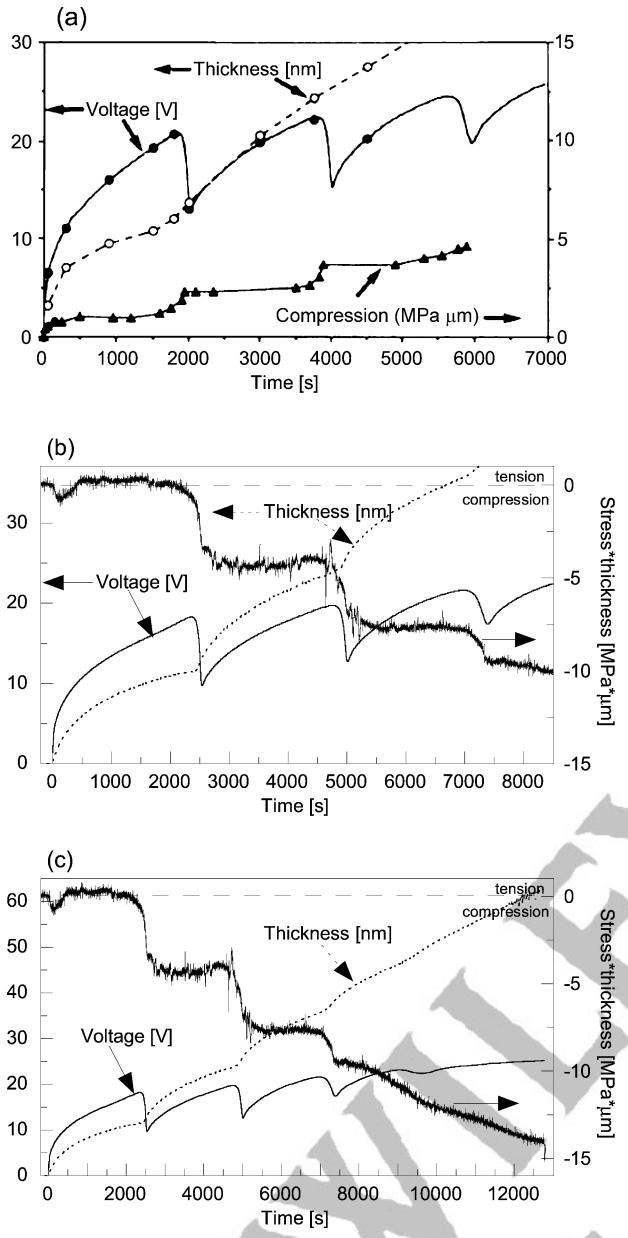

Figure 1. Evolution of the cell potential, oxide thickness and stress*thickness ■* OK?■ product with time during galvanostatic anodising of silicon at 0.10 mA cm^{-2} in 10% acetic acid. Lehmann's original experiment (a)[13] is compared with our own reproduction on similar ordinate and abscissa scales (b), as well as for the full duration of the experiment carried out until oscillations are damped (c).

tive index spectra of our anodic silica films. For a wavelength of 633 nm, they are equal to 1.438, 1.434 and 1.409 for anodic silica grown at 0.07, 0.13 and 1.0 mA cm^{-2}, respectively.

The simultaneous monitoring of the cell potential and thickness also allows analysis of the evolution of the electric field $E = V/h_f$ across the oxide film. Figure 4 shows, for the same current densities as in Figure 2, the evolution of both the cell potential and electric field with respect to oxide thickness. As in Figure 3, the first thickness transition has been indicated by a dashed vertical line. From the more or less constant slopes in Figure 4a in between the transitions during most of the anodic growth process, the electric field is seen to remain constant. However, during the transition itself, the field decreases rather abruptly, mainly due to the sudden voltage drop (cf. Figure 3).

From a mechanical point of view, Figure 1 already showed a systematic increase of the internal stress in the compressive direction during the spontaneous voltage drops at the transition. To confirm the consistency of the sign of the stress change in the compressive direction associated with the voltage drops, an additional experiment was performed in which the current was intentionally switched off before the first spontaneous potential drop was allowed to occur. The associated curvature evolution is shown in Figure 5, and indeed confirms a stress change in the compressive direction during such an imposed voltage drop upon current switch-off, even if the initial stress state is tensile. The fact that the internal stress in the oxide at the voltage drops (spontaneous or imposed) was always observed to change in the compressive direction (i.e. from compressive to more compressive, or from tensile to compressive) has already some important consequences as to the possible mechanical origin of the oscillations. Indeed, it allows one to exclude the hypothesis of a mechanical relaxation accompanying the transition. In other words, the transition cannot be stress-induced, contrary to what has been assumed by Lehmann, but induces itself a change in the internal stress evolution.

Continuing our search for the origin of the correlated voltage and stress transitions, we then performed detailed cross-sectional TEM characterisations on silica films anodised at 0.10 mA cm^{-2} for, respectively, 6800 and 12800 s. This corresponds to sample thicknesses that are either still within the oscillatory regime, or after damping at the end of the experiment (see Figure 1c).

Figure 6 shows cross-sectional high-resolution TEM (HRTEM) images obtained from FIB lamellae prepared from the two silica layers. The thickness of these layers is equal to about 64 and 32 nm, respectively, in good agreement with the in situ ellipsometric thickness data of Figure 1c. Both images show a homogeneous silica layer covering the crystalline Si substrate. The Fourier transform (FT) patterns shown as insets confirm that the layers are fully amorphous: only diffuse rings can be seen in the FT patterns, whereas spots indicating the presence of any crystallographic periodicity are not observed. It is worth mentioning here that, although regular porosity within the silica layers is not visible in the HRTEM images of Figure 6, the presence of slight variations in sample thickness due to, for example, small voids cannot be fully excluded from these micrographs. Therefore, to ascertain whether or not any small pores or holes are present in the silica film, the HAADF-STEM technique was used. This allows the display of the so-called mass–thickness image contrast. Figure 7a and c are high-resolution cross-sectional HAADF-STEM images obtained from the 32 and 64 nm thick silica layers, respectively. Image intensity profiles, taken over the full width of the *Z*-contrast images, are also displayed. The profiles confirm that the thickness of the layers is almost constant. Only a slight decrease in thickness close the surface of the two silica layers can be observed, which can be

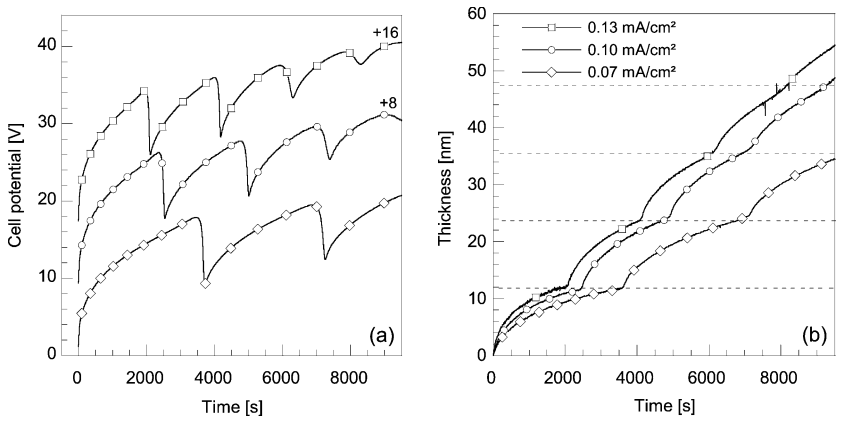

Figure 2. Time evolution of the cell potential (a) and anodic oxide thickness (b) during galvanostatic anodising of silicon in 10% acetic acid at current densities of 0.13 (squares), 0.10 (circles) and 0.07 mA cm^{-2} (diamonds). For clarity reasons, potential curves at 0.13 and 0.10 mA cm^{-2} have been shifted upwards by 16 and 8 V, respectively.

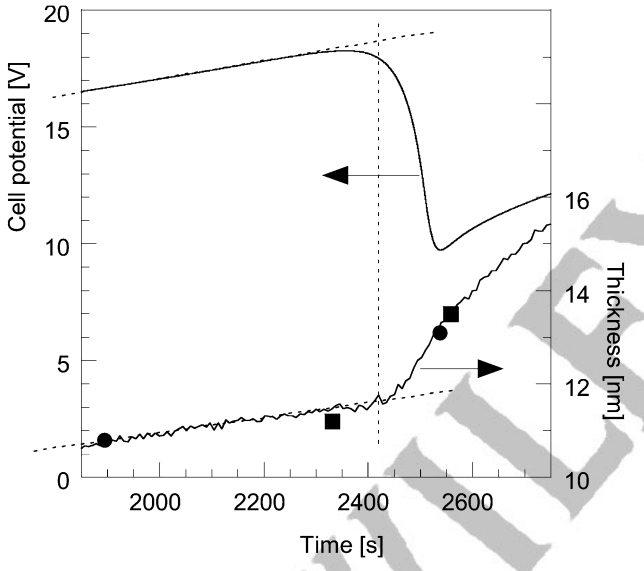

Figure 3. Enlargement of the potential and thickness evolution of Figure 1 around the first transition. The dashed vertical line visualises a significant time-shift between the onset of the voltage and thickness transitions. The thickness evolution is also compared with ex situ thickness measurements performed by Lehmann (circles) and Parkhutik (squares) on galvanostatically anodised silica.[9,13] These ex situ measurements have been relocated onto our own experimental timescale by keeping the same relative position within one cycle.

attributed to the FIB thinning during sample preparation. Therefore, these results exclude the presence of porosity in the form of nanosized cracks or voids with dimensions superior to 0.5–1 nm. The composition of the films was also analysed by spatially resolved STEM-EELS. The scans shown in Figure 7 b and d indicate a perfect SiO_2 stoichiometry across the entire thickness of the two layers. The latter findings also agree with compositional results obtained by Parkhutik from infrared spectroscopy in the regime of damped oscillations.[16]

These complementary ex situ characterisations therefore allow us to conclude that the oscillatory behaviour, besides not being stress-induced, is not based on a morphological transition either. In this respect, it should be recognised though that Lehmann's paper considered two possible and seemingly independent morphological transitions: an increase in surface roughness, as derived from ex situ plane-view AFM (cf. his Figure 5 in ref. [13]), and a dense-to-porous transition, only assumed indirectly from fitting X-ray reflection spectra (cf. the bar graph sketch in his Figure 3, ref. [13]). At this stage, we can only reliably exclude the second, dense-to-porous morphological transition. Note that the latter also justifies our initial assumption of a constant refractive index during oxide growth.

To address the question of a possible morphological transition occurring at the surface, we also performed a detailed AFM surface characterisation on our own anodic silica samples at different growth stages. Results for the sample root-mean-square (RMS) roughness are shown in Figure 8 in relation to the temporal evolution of the cell voltage, to address any possible link with the electrochemical oscillations. The data show an overall steady increase of the surface roughness during growth, as can be expected for a thin film with continuously increasing thickness. However, directly after the transition, a relatively small decrease in roughness is observed, on the order of only 3.6 and 5.0% after the first and second transition, respectively. These results are therefore in disagreement with Lehmann's claim that the transitions can be associated with an increase of the surface roughness. However, we should point out that Lehmann might have missed the roughness decrease at the transition, because he did not characterise a sample anodised up to the onset of transition (see measurement points A and B indicated in his Figure 3[13]). In any case, the evolution of the surface roughness gives in our opinion no indication of the existence of a morphological transformation at the surface of the oxide film, since it increases when the oxide thickens, as can simply be expected for a continuously growing thin film.

3. Discussion

Our own experimental evidence provided above disagrees rather fundamentally with the two main hypotheses formulated by Lehmann in his original paper regarding the nature of the transitions underlying the oscillation process during Si anodising: first of all, the transition is not stress-induced, and secondly it is not a morphological one. In our opinion, these new findings therefore also require that existing modelling efforts trying to advance the understanding of electrochemical oscillations at silicon electrodes and based on such stress-induced morphological transitions,[9,11,12] need to be revised. On

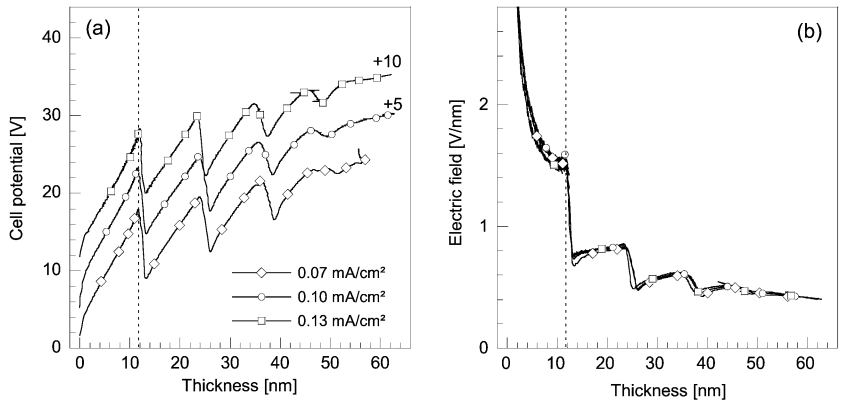

Figure 4. Evolution of the cell potential (a) and electric field (b) with respect to oxide thickness for anodic silica grown at 0.13 (squares), 0.10 (circles) and 0.07 mA cm^{-2} (diamonds). The position of the dashed vertical line, which identifies the first transition, is identical to that in Figure 3. For clarity reasons, potential curves at 0.13 and 0.10 mA cm^{-2} have been shifted upwards by 10 and 5 V, respectively.

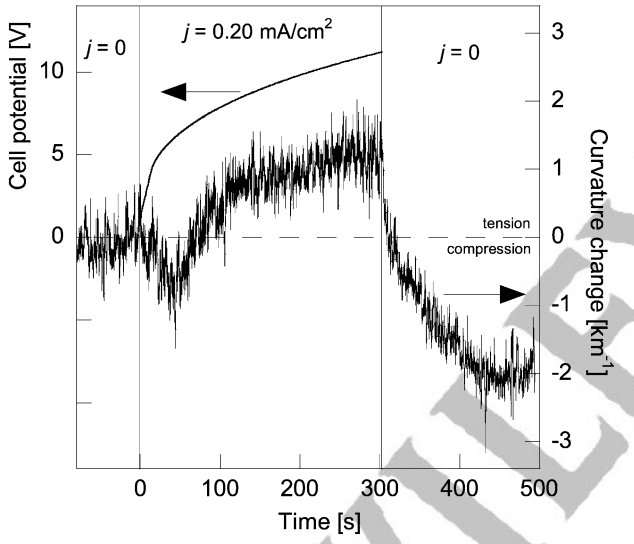

Figure 5. Curvature evolution before the first potential transition during Si anodising at 0.20 mA cm^{-2}. After the anodic current is switched off after 300 s, the curvature changes in the compressive direction.

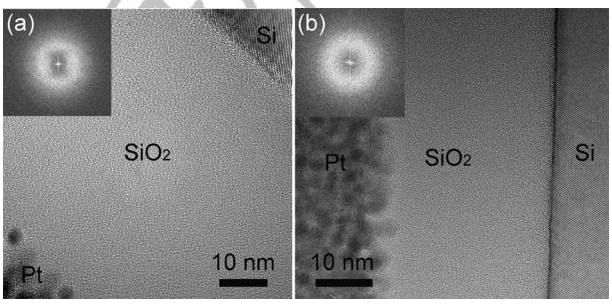

Figure 6. Cross-sectional HRTEM images obtained from FIB lamellae prepared from the silica layers anodised at 0.10 mA cm^{-2} for a) 12 800 and b) 6800 s. Both the silicon substrate and the protective electron-beam-deposited Pt layer can be seen in the images. Insets: The rings present in the FTs obtained in the SiO_2 regions confirm the fully amorphous character of the silica layers.

the other hand, it does leave us with two as yet unanswered questions: firstly, what causes the observed systematic increase of the internal stress in the compressive direction during the transitions, and secondly, what is then the alternative nature of the transitions underlying the oscillations, if not a morphological transformation of the film?

With respect to the mechanical aspect, we already pointed out in Figure 4 that from an electrochemical perspective, the transitions are characterised by a rather abrupt and significant decrease in the electrical field. As the evolution of the internal stress was shown to be the result (and not the cause) of such a transition, it can be expected that it is the electric-field-induced or so-called electrostrictive component of the internal stress that is affected at the transition. This also agrees with the observation in Figure 3 that the oxide thickness during the transition remains relatively constant. The latter indeed implies that the growth-induced internal stress component, which results from a thickness increase of anodised silicon either at the electrolyte or substrate side, stays unaffected. We have already performed a number of dedicated experimental studies in the past unravelling the contribution of electrostriction as a reversible, field-induced component of the total internal stress in anodic oxide films.[14,17,18] In short, the application of an electric field to a dielectric induces a reversible electrostatic stress, which encompasses two distinct though interlinked contributions. The first one, usually referred to as the Maxwell stress, results from the Coulombic attraction between charges of opposite sign located on both sides of the dielectric. The in-plane component of the Maxwell stress in a thin oxide film submitted to a homogeneous field E perpendicular to the oxide plane can be assessed by using a simple parallel-plate capacitor model and varies quadratically with the electric field according to [Eq. (2)]:

$$\sigma_{ES}^{*} = -\left(\frac{1}{1-\nu}\right) \cdot \frac{\varepsilon_0 \varepsilon}{2} \cdot E^2 \qquad (2)$$

in which ν is the Poisson coefficient of the oxide film, ε its relative dielectric constant at zero stress and ε_0 the vacuum permittivity. The minus sign in Equation (2) indicates that the in-plane Maxwell stress is compressive in the thin-film geometry as a result of the Coulombic attraction along the thickness direction.

Besides the Maxwell stress, a second contribution to electrostriction arises from the effect of a field-induced dipole alignment on the permittivity of the dielectric. This effect is sometimes referred to as dielectrostriction, so as to avoid confusion with the overall electrostriction stress. The alignment of di-

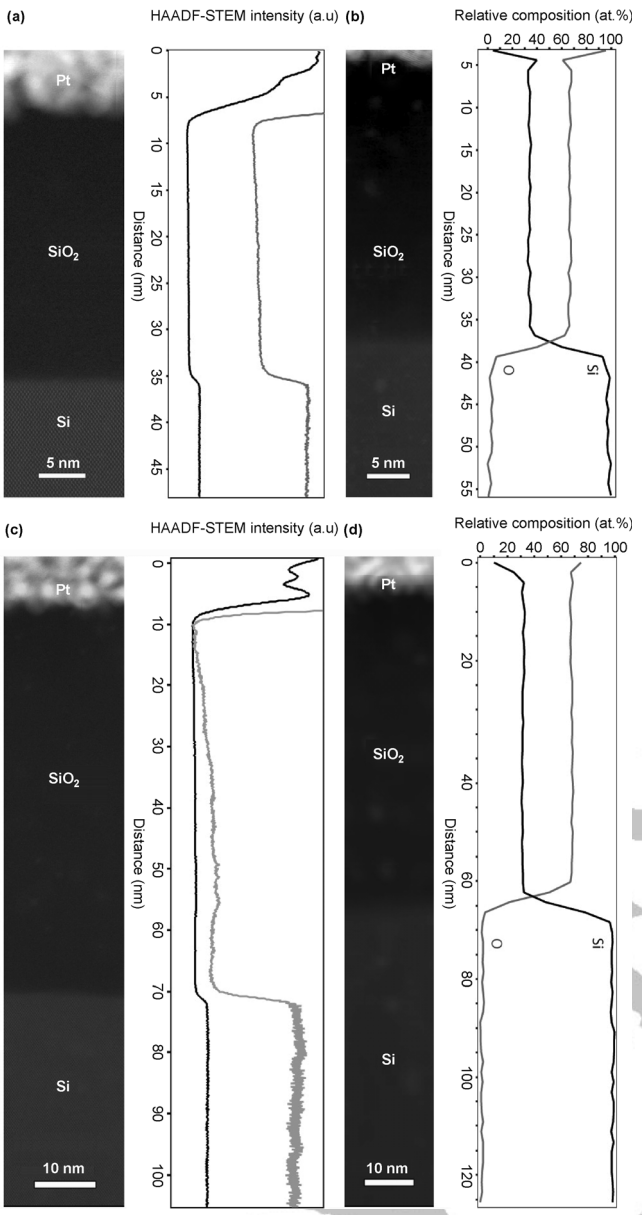

Figure 7. a) Cross-sectional HAADF-STEM image obtained on the 32 nm thick silica layer anodised for 6800 s, together with HAADF intensity profiles over the image (grey line: enhanced contrast). b) Cross-sectional HAADF-STEM image obtained from the same silica layer, together with the relative compositions of Si and O obtained from a STEM-EELS scan over the layer. c) Cross-sectional HAADF-STEM image and intensity profile for the 64 nm thick silica layer anodised for 12800 s. d) Cross-sectional HAADF-STEM image obtained from the same silica layer, together with relative compositions of Si and O obtained from STEM-EELS.

poles along the direction of the applied field and the resulting deformation of the dielectric induces a modification of its permittivity, as described by the Clausius–Mosotti theory. Contrary to what is often being claimed in the literature, this second contribution to the overall field-induced electrostriction stress is far from being negligible.[19] The effect of dielectrostriction can be taken into account through the use of two electrostriction parameters α_1 and α_2. A detailed treatment can be found in the works of Lee, McMeeking and Suo,[19–21] which are all

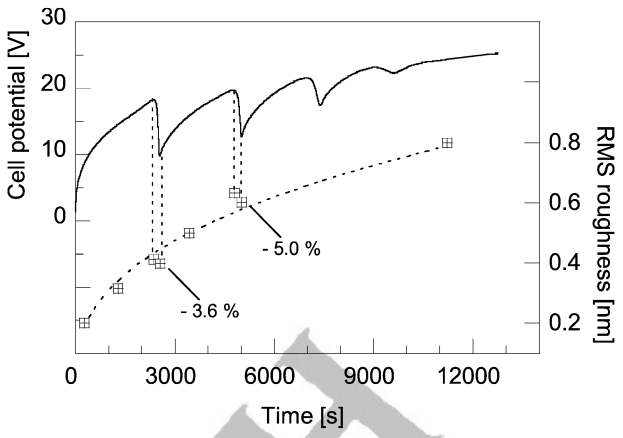

Figure 8. Time evolution of the surface roughness as measured ex situ by AFM on samples anodised to different growth stages, as testified by the superimposed cell voltage evolution. The dashed line is simply a guide to the eye.

based on the original work of Landau and Lifshitz.[22] From their results, the in-plane electrostriction stress σ_{ES} resulting from a field E along the thickness of a dielectric film attached to a substrate can be expressed as [Eq. (3)]:[14]

$$\sigma_{ES} = -\frac{\varepsilon_0 \cdot E^2}{2} \cdot (\varepsilon(1+\nu) - \alpha_1 \nu + \alpha_2(1-\nu)) \quad (3)$$

Note that this modified Equation (3) is formally very similar to the simplified Equation (2) for the Maxwell stress only, including the quadratic field dependence. However, it takes into account explicitly the contribution from dielectrostriction through the use of the two electrostriction parameters α_1 and α_2, which for linearly isotropic dielectrics can be further expressed as a function of their permittivity.[17]

The importance of electrostriction Equation (3) for the present work is two-fold. First of all, we have already shown before[14] that specifically in the case of anodic silica, the electrostrictive stress component takes on a tensile sign, thereby reversing the generally (but wrongly) accepted compressive contribution coming from the Maxwell stress alone. As a result, a decreasing or vanishing electrical field will necessarily induce a decrease of the tensile, electrostrictive stress component of the total internal stress. The latter will therefore necessarily increase (instead of relax) in the compressive direction. This is qualitatively fully consistent with our own and Lehmann's mechanical observations accompanying the transitions, as shown in Figure 1. Moreover, quantitatively, these internal stress changes during the transitions should then, according to the electrostriction Equation (3), vary quadratically with the electrical field. Figure 9 illustrates that this is indeed verified for the first two transitions at all different current densities being tested. For a fixed current density, Figure 9 also reveals an increase in slope of the $\sigma - E^2$ curves during the transitions in the course of anodising. According to Equation (3), this would be indicative of a change in the dielectric behaviour of the anodic silica, most likely through a change in its electrostriction cou-

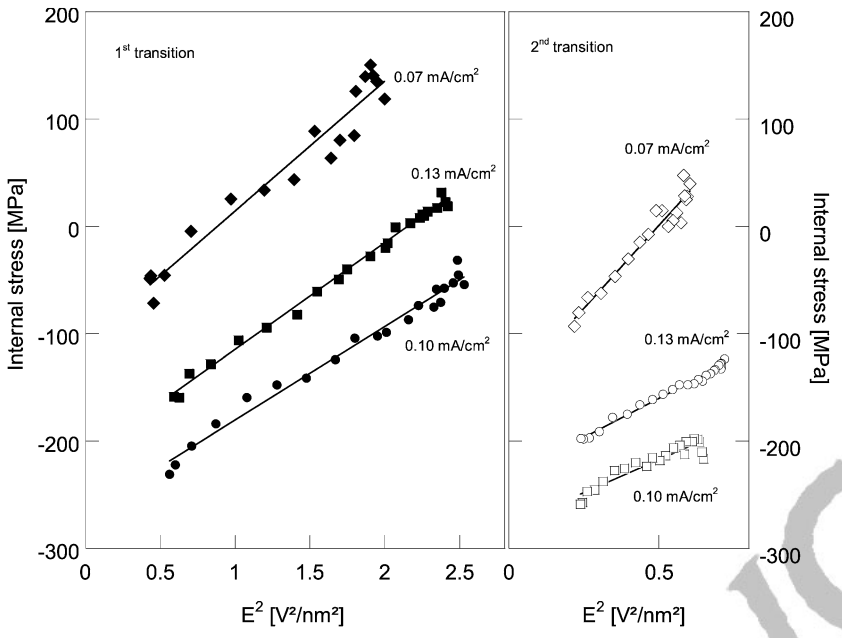

Figure 9. Correlation between the magnitude of the internal stress and the square of the electric field during the first (left) and second (right) transition at each of the current densities, validating Equation (3). For the third and fourth transitions, not enough data points were available to justify a reliable fit.

pling parameters α_1 and α_2 and/or their constitutive variation with ε, which at this stage remains as yet unresolved.

The second remaining open question is related to the nature of the transition itself underlying the oscillations. We believe that the abrupt and significant decrease in electrical field at the transition, which results from a rather steep drop in potential at nearly constant thickness, points towards an electrical origin. We thereby tend to be in line with a recent study suggesting that the oscillations do indeed have an electrical origin, rather than a morphological one.[23] A relevant additional experiment in this respect is shown in Figure 10, which aims to address the effect of an imposed, intermittent oxide depolarisation during the anodic growth process. In this experiment, the anodic current (set to yield $j = 0.10\ \mathrm{mA\,cm^{-2}}$) was switched off at about 16 V (or 11 nm), that is, well before the first spontaneous oscillation would occur, and the subsequent voltage decrease during oxide depolarisation was recorded. Then, after a well-defined time interval, the current was switched back on again, and the new voltage and thickness evolutions were monitored. In Figure 9■■Figure 10?■■, two different situations are depicted, depending on the duration of intermittent oxide depolarisation. For an almost instantaneous depolarisation (Figure 10,■■OK?■■ < 2 s, squares), the effect of a current switch-off is negligible: the cell voltage quickly resumes its pre-interruption value and the growth rate is not affected. In this case, the thickness and electric field at the subsequent first spontaneous transition are equal to 12.7 and 1.6 $\mathrm{V\,nm^{-1}}$, respectively. These values are very similar to those in the case of the continuous growth process already shown in Figure 2. However, if the current switch-off takes longer (Figure 10■■OK?■■, > 5 s, circles on dashed line), the imposed depolarisation triggers the start of a new, imposed oscillation. In the latter case, the thickness and the electric field at the subsequent first spontaneous transition are equal to, respectively, 22.5 nm and 0.9 $\mathrm{V\,nm^{-1}}$.

This experiment demonstrates first of all that the moment when a spontaneous transition occurs is independent of the absolute thickness or the magnitude of the electric field. In line with the observations of Figure 2, it rather seems to be related to the accumulated amount of charge that has passed: about 230 $\mathrm{mC\,cm^{-2}}$ or 12.7 nm per cycle for the instantaneous current switch-off, and about 180 $\mathrm{mC\,cm^{-2}}$ or 11 nm for the longer one.

Secondly, the characteristic features of the transition in terms of voltage and thickness

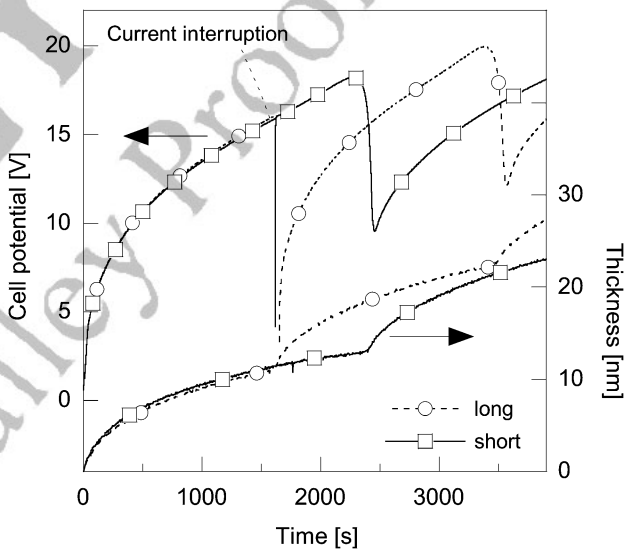

Figure 10. Evolution of the cell potential and oxide thickness during silicon anodising at 0.10 $\mathrm{mA\,cm^{-2}}$ with an imposed current interruption at 16 V. The current has been switched off for 1.7 s (squares) and 4.7 s (circles on dashed line).

evolution can be fully reproduced by a depolarisation of the oxide film during current switch-off. We therefore attribute the origin of the transition to a sudden dissipation of the accumulated charges. A related although not fully equivalent mechanism has been proposed by Föll et al.[24] They rather used the term "breakdown" and imagined the transition being triggered by a critical electric field. However, as we found the spontaneous transitions to occur independently of the magnitude of

the electric field, the term breakdown does not seem fully justified in our opinion. We rather adhere to the viewpoint of Chazalviel[25] who, based on detailed transient current and capacitance measurements, proposed a build-up and storage of positive and negative charges at, respectively, the silicon and electrolyte interface under anodic polarisation. His description of ionic processes occurring during anodic silica growth is also in agreement with our observation of oxide growth being inhibited or resumed just before or after the transition, respectively. Indeed, during growth under anodic polarisation, charged species will gradually accumulate at both sides of the oxide film, the resulting polarisation thereby progressively inhibiting ionic motion by local buffering of the electric field. As a result, the oxide growth rate gradually slows down, until the accumulated charges (spontaneously) dissipate and the growth rate increases again. Such a cumulative injection of charges has already been shown in the past to be a possible trigger for electrical breakdown,[26,27] the latter term being associated in these cases with the degradation of the oxide's dielectric properties.[28] We prefer to avoid the misleading term breakdown, which suggests a field-dependence, and rather associate the oscillations with a cyclic depolarisation of the anodic silica film, spontaneous or imposed, after a critical amount of charge has passed. The resulting charge dissipation then causes a drop in voltage (and field), after which the initial growth dynamics can resume again.

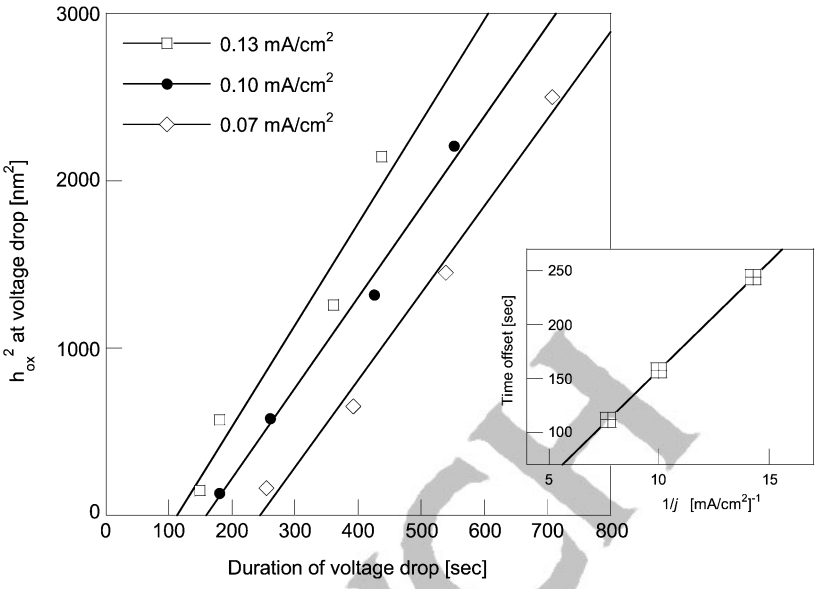

Figure 11. Correlation between the square of the oxide thickness and the duration of the voltage drop for all oscillations. Anodising performed at 0.13 (squares), 0.10 (circles) and 0.07 mA cm^{-2} (diamonds).

Note that the above observation that the amount of charge passing before a spontaneous transition is lower during the imposed current switch-off than for the uninterrupted experiment also complies with the above-described general mechanistic framework. Indeed, when linking the oscillations to a periodic electrical discharging of the oxide, we can imagine the intermediate, external switching off and back on of the current to result in an incomplete depolarisation of the oxide. As a result, some charges would still remain in the film and give a "head start" for the next critical charge accumulation.

A final step towards a full understanding of the electrochemical oscillations is then intimately linked to the fundamental understanding of the charge dissipation mechanism. According to Chazalviel,[25] the dissipation of charges in the transient regime, that is, without externally applied field, is accomplished by backward migration of positive charges into the silicon. However, in our own galvanostatic experiments, the direction of the residual electric field can be expected to prevent charges, at least partially, from migrating backward. We therefore rather adhere to the possibility of a diffusion-controlled charge dissipation mechanism across the entire oxide thickness. This hypothesis originates from the observation in Figure 11 that, at constant current density, the duration of the voltage drop increases proportionally to the square of the nominal oxide thickness at which each oscillation occurs. Moreover, from the statistically identical slopes in Figure 10, a constant diffusion coefficient on the order of 10^{-14} cm^2 s^{-1} is obtained for the main dissipating charges, independent of current density. The fact that this value is much lower than the one reported for the diffusion of charged oxygen in silica (on the order of 10^{-7} cm^2 s^{-1}, taking a pre-exponential factor of 8×10^{-3} cm^2 s^{-1}[29] and an activation energy of 0.27 eV[30]) suggests either that species other than oxygen anions are responsible for charge dissipation, in line with the findings of Chazalviel, or that backward diffusion of charged species is partly inhibited by the residual electric field, in agreement with the early work of Jorgensen.[31] An interesting additional observation in this respect are the non-zero, positive intercepts at the abscissa in Figure 11, which can be taken as indicative of a time delay between the beginning of the voltage drop and the beginning of the diffusion process. As shown in the inset of Figure 11, these time offsets were found to increase with decreasing current density, according to $1/j$. We do recognise that a complete understanding of the details of the charge dissipation mechanism and therefore also the oscillation process clearly still needs additional attention. Nonetheless, we believe it provides at this stage a rather elegant explanation for their characteristic damping observed in fluoride-free media, dissipation being increasingly slowed down as the oxide thickens.

4. Conclusions

We have addressed the origin of damped electrochemical oscillations at silicon anodes by combining high-resolution in situ

stress and thickness measurements with a detailed ex situ morphological and structural characterisation using high-resolution cross-sectional TEM. As such, we have been able on the one hand to carefully reproduce Lehmann's original experimental findings as reported in ref. [13], but on the other hand to disprove his claim of a stress-induced morphological transition. Instead, we have attributed the periodic stress transitions in the compressive direction to variations in the tensile, field-induced electrostrictive stress component in the silica film, which results from a periodically relaxing electrical field inside the anodic silica film. The origin of the oscillations is believed to be electrical in nature, which we imagine as a periodically re-occurring, diffusion-controlled charge dissipation mechanism across the entire oxide thickness. Moreover, we found the transitions, spontaneous or imposed, to occur after a critical amount of charge had passed, independently of the magnitude of the electric field.

Acknowledgements

This work has been supported by the European Union and Walloon Region FEDER grant ECP12020021680F. J.P. and H.I. also acknowledge support of the Belgian Interuniversity Attraction Poles (IAP) under contract No. P7/21. We cordially thank Bernard Nysten for his help with the AFM measurements.

Keywords: anodizing · molecular electrochemistry · oscillations · silicon · stress

[1] V. Parkhutik, *Solid-State Electron.* **2001**, *45*, 1451 – 1463.
[2] H. Lewerenz, M. Aggour, *J. Electroanal. Chem.* **1993**, *351*, 159 – 168.
[3] F. Ozanam, J.-N. Chazalviel, A. Radi, M. Etman, *J. Electrochem. Soc.* **1992**, *139*, 2491 – 2501.
[4] I. Miethe, K. Krischer, *J. Electroanal. Chem.* **2012**, *666*, 1 – 10.
[5] S. Böhm, L. M. Peter, G. Schlichthörl, R. Greef, *J. Electroanal. Chem.* **2001**, *500*, 178 – 184.
[6] J.-N. Chazalviel, C. da Fonseca, F. Ozanam, *J. Electrochem. Soc.* **1998**, *145*, 946 – 973.
[7] S. Cattarin, F. Decker, D. Dini, B. Margesin, *J. Electroanal. Chem.* **1999**, *474*, 182 – 187.
[8] D. Dini, S. Cattarin, F. Decker, *J. Electroanal. Chem.* **1998**, *446*, 7 – 11.
[9] V. Parkhutik, Y. Chu, H. You, Z. Nagy, P. A. Montano, *J. Porous Mater.* **2000**, *7*, 27 – 31.
[10] F. Decker, E. Pantano, D. Dini, S. Cattarin, S. Maffi, G. Razzini, *Electrochim. Acta* **2000**, *45*, 4607 – 4613.
[11] J.-N. Chazalviel, R. Cortès, F. Maroun, F. Ozanam, *Phys. Status Solidi A* **2009**, *206*, 1229 – 1234.
[12] J. Grzanna, T. Notz, H. J. Lewerenz, *Phys. Status Solidi C* **2009**, *6*, 1639 – 1643.
[13] V. Lehmann, *J. Electrochem. Soc.* **1996**, *143*, 1313 – 1318.
[14] F. Blaffart, Q. Van Overmeere, T. Pardoen, J. Proost, *J. Solid State Electrochem.* **2013**, *17*, 1945 – 1954.
[15] Q. Van Overmeere, J.-F. Vanhumbeeck, J. Proost, *Rev. Sci. Instrum.* **2010**, *81*, 045106.
[16] V. P. Parkhutik, *Electrochim. Acta* **1991**, *36*, 1611 – 1616.
[17] J.-F. Vanhumbeeck, J. Proost, *Electrochim. Acta* **2008**, *53*, 6165 – 6172.
[18] Q. Van Overmeere, F. Blaffart, F. La Mantia, F. Di Quarto, J. Proost, *J. Appl. Phys.* **2012**, *111*, 113529.
[19] H. Y. Lee, Y. Peng, Y. M. Shkel, *J. Appl. Phys.* **2005**, *98*, 074104.
[20] R. M. McMeeking, C. M. Landis, *J. Appl. Mech.* **2005**, *72*, 581 – 590.
[21] X. Zhao, Z. Suo, *J. Appl. Phys.* **2008**, *104*, 123530.
[22] L. D. Landau, E. M. Lifshitz, *Electrodynamics of Continuous Media*, Pergamon, Oxford, **1960**.
[23] K. Schönleber, K. Krischer, *ChemPhysChem* **2012**, *13*, 2989 – 2996.
[24] E. Foca, J. Carstensen, H. Föll, *J. Electroanal. Chem.* **2007**, *603*, 175 – 202.
[25] J.-N. Chazalviel, *Electrochim. Acta* **1992**, *37*, 865 – 875.
[26] M. Nafría, J. Suñé, X. Aymerich, *Microelectron. Reliab.* **1996**, *36*, 871 – 905.
[27] D. J. Dimaria, *Solid-State Electron.* **1997**, *41*, 957 – 965.
[28] J. F. Verweij, J. H. Klootwijk, *Microelectron. J.* **1996**, *27*, 611 – 622.
[29] S. Kostinski, R. Pandey, S. Gowtham, U. Pernisz, A. Kostinski, *IEEE Electron Device Lett.* **2012**, *33*, 863 – 865.
[30] Y.-G. Jin, K. J. Chang, *Phys. Rev. Lett.* **2001**, *86*, 1793 – 1796.
[31] P. J. Jorgensen, *J. Chem. Phys.* **1962**, *37*, 874 – 877.

Received: April 4, 2014
Revised: May 27, 2014
Published online on ■■ ■■, 0000

ARTICLES

J. Proost, F. Blaffart, S. Turner, H. Idrissi*

■■ – ■■

On the Origin of Damped Electrochemical Oscillations at Silicon Anodes (Revisited)

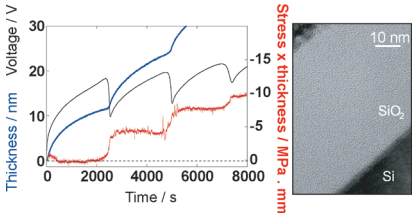

Seeing is believing: A widely accepted model of oxide growth during galvanostatic anodizing of Si in fluoride-free electrolytes is questioned by revisiting the underlying seminal experiment carried out about two decades ago. As such, the fundamental hypothesis of a stress-induced morphological transition of the anodic oxide accompanying the damped electrochemical oscillations is disproven. ■■ The figure was too large; change OK? ■■

Damped #electrochemical oscillations at #silicon #anodes revisted @UCLouvain be @UAntwerpen SPACE RESERVED FOR IMAGE AND LINK

ChemPhysChem is piloting a social networking feature involving Twitter, an online microblogging service that enables its users to send and read text-based messages of up to 140 characters, known as "tweets". Please check the pre-written tweet in the galley proofs for accuracy. Should you or your institute have a Twitter account, please let us know the appropriate username (e.g., @ChemPhysChem), and we will do our best to include this information in the tweet. This tweet will be posted to the journal's Twitter account upon online publication of your article.